

## Germline Missense Mutations Affecting KRAS Isoform B Are Associated with a Severe Noonan Syndrome Phenotype

Claudio Carta, Francesca Pantaleoni, Gianfranco Bocchinfuso, Lorenzo Stella, Isabella Vasta, Anna Sarkozy, Cristina Digilio, Antonio Palleschi, Antonio Pizzuti, Paola Grammatico, Giuseppe Zampino, Bruno Dallapiccola, Bruce D. Gelb,\* and Marco Tartaglia\*

Noonan syndrome (NS) is a developmental disorder characterized by short stature, facial dysmorphism, congenital heart disease, and multiple skeletal and hematologic defects. NS is an autosomal dominant trait and is genetically heterogeneous. Gain of function of SHP-2, a protein tyrosine phosphatase that positively modulates RAS signaling, is observed in nearly 50% of affected individuals. Here, we report the identification of heterozygous *KRAS* gene mutations in two subjects exhibiting a severe NS phenotype with features overlapping those of cardiofaciocutaneous and Costello syndromes. Both mutations were de novo and affected exon 6, which encodes the C-terminal portion of KRAS isoform B but does not contribute to KRAS isoform A. Structural analysis indicated that both substitutions (Val152Gly and Asp153Val) perturb the conformation of the guanine ring-binding pocket of the protein, predicting an increase in the guanine diphosphate/guanine triphosphate (GTP) dissociation rate that would favor GTP binding to the KRASB isoform and bypass the requirement for a guanine nucleotide exchange factor.

Noonan syndrome (NS [MIM 163950]) is a clinically variable disorder defined by short stature, facial dysmorphism, multiple skeletal defects, and congenital heart disease.<sup>1-3</sup> The distinctive facial features consist of a broad forehead, hypertelorism, down-slanting palpebral fissures, high-arched palate, and low-set, posteriorly rotated ears. Cardiac involvement is present in up to 90% of affected individuals, with pulmonic stenosis, hypertrophic cardiomyopathy, atrioventricular septal defects, and aortic coarctation representing the most common lesions.<sup>4</sup> Additional relatively recurrent features of NS are webbed and/or short neck, mental retardation, cryptorchidism, and hematologic anomalies. Although precise epidemiological data are not available, the prevalence of NS is estimated to be between 1 in 1,000 and 1 in 2,500 live births.<sup>5</sup>

NS is an autosomal dominant trait and is genetically heterogeneous.<sup>6</sup> Using a positional candidacy approach, we established *PTPN11* as the NS disease gene residing at *NS1* (12q24),<sup>7</sup> and studies by our groups and others have demonstrated that mutations in *PTPN11* account for nearly 50% of affected individuals.<sup>5</sup> The *PTPN11* gene encodes the cytoplasmic protein tyrosine phosphatase SHP-2, a widely expressed signal transducer with crucial roles in the cellular response to growth factors, hormones, and cytokines.<sup>8</sup> Accumulating genetic, modeling, and biochemical data indicate that NS-causing *PTPN11* mutations promote SHP-2 gain of function.<sup>7,9-12</sup> In contrast, a limited

number of germline *PTPN11* missense mutations that seem to engender dominant negative effects cause the phenotypically related LEOPARD syndrome (MIM 151100).<sup>12-15</sup> Finally, a distinct class of somatic *PTPN11* mutations promoting stronger activation of SHP-2 has been identified as contributing to leukemogenesis.<sup>11,12,16-18</sup>

SHP-2 is an essential component of the machinery required for the activation of the RAS-mediated intracellular signaling pathways, and converging data indicate that germline and somatic *PTPN11* mutations cause deregulation of RAS function.<sup>15,16,19-22</sup> RAS proteins act as GDP/GTP-regulated molecular switches to control intracellular signal flow.<sup>23,24</sup> They exhibit high affinity for both GDP and GTP and low GTPase activity. GDP/GTP cycling is controlled by GTPase-activating proteins (GAPs), which accelerate the intrinsic GTPase activity, and by guanylyl-exchanging factors (GEFs), which promote release of GDP. RAS proteins cycle from a GDP-bound inactive state to a GTP-bound active state, the latter allowing signal flow by protein interaction with multiple downstream transducers. RAS proteins share a structure that includes a conserved domain (residues 1-165), known as the "G domain," which is required for signaling function, and a less conserved C-terminal tail, called the "hypervariable region," that guides posttranslational processing and plasma membrane anchoring (fig. 1A). Within the conserved region, five motifs (G-1 to G-5) direct the GTP/GDP binding

From the Dipartimento di Biologia Cellulare e Neuroscienze, Istituto Superiore di Sanità (C.C.; F.P.; M.T.), Dipartimento di Scienze e Tecnologie Chimiche, Università di Roma "Tor Vergata" (G.B.; L.S.; A. Palleschi), Istituto di Clinica Pediatrica, Università Cattolica del Sacro Cuore (I.V.; G.Z.), Dipartimento di Medicina Sperimentale e Patologia, Università "La Sapienza" and Istituto CSS-Mendel (A.S.; A. Pizzuti; B.D.), Genetica Medica, Ospedale "Bambino Gesù" (C.D.), and Genetica Medica, Dipartimento di Medicina Sperimentale e Patologia, Università "La Sapienza," Azienda Ospedaliera S. Camillo-Forlanini (P.G.), Rome; IRCCS-CSS, San Giovanni Rotondo, Italy (A.S.; A. Pizzuti; B.D.); and Departments of Pediatrics and Human Genetics, Mount Sinai School of Medicine, New York (B.D.G.)

Received February 8, 2006; accepted for publication March 14, 2006; electronically published May 1, 2006.

Address for correspondence and reprints: Dr. Marco Tartaglia, Istituto Superiore di Sanità, Dipartimento di Biologia Cellulare e Neuroscienze, Viale Regina Elena 299, 00161 Rome, Italy. E-mail: mtartaglia@iss.it

\* These two authors contributed equally as the senior investigators for this project.

*Am. J. Hum. Genet.* 2006;79:129-135. © 2006 by The American Society of Human Genetics. All rights reserved. 0002-9297/2006/7901-0014\$15.00

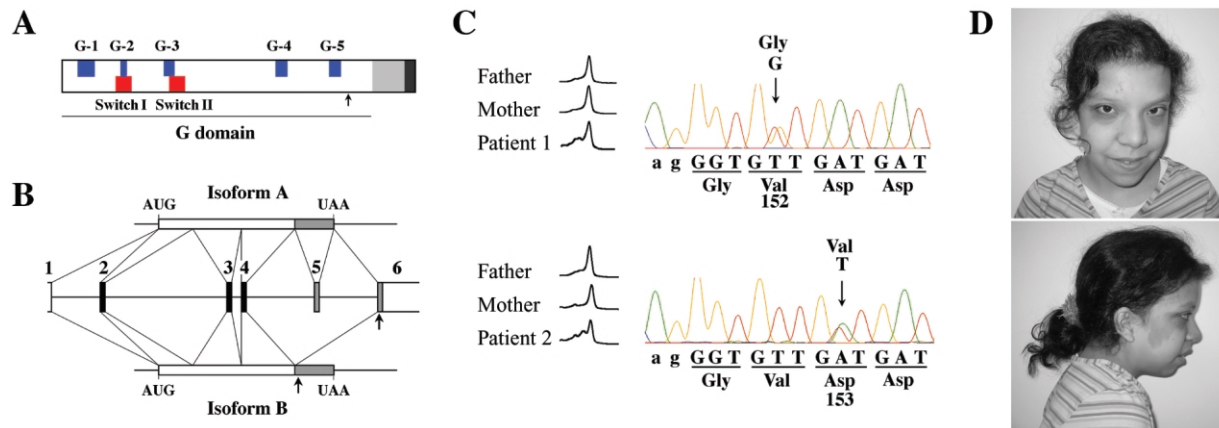


**Figure 1.** Heterozygous *KRAS* missense mutations causing a severe Noonan syndrome phenotype with features overlapping those of CFC and CS. *A*, Schematic representation of the structural and functional domains defined within RAS proteins.<sup>25</sup> The conserved domain (G domain) is indicated, together with the motifs required for signaling function. The hypervariable region is shown (gray), as is the C-terminal motifs that direct posttranslational processing and plasma membrane anchoring (dark gray). The arrow indicates the location of affected residues. *B*, *KRAS* gene organization and transcript processing that produces the alternative *KRAS* isoforms A and B (Gene accession numbers NC\_000012, NM\_004985, and NM\_033360). The numbered black and gray boxes indicate the invariant coding exons and the exons undergoing alternative splicing, respectively. *KRASB* mRNA results from exon 5 skipping. In *KRASA* mRNA, exon 6 encodes the 3' UTR. The arrows indicate locations of mutations. *C*, DHPLC elution profiles (left) and electropherograms (right) of *KRAS* exon 6 PCR products showing the de novo heterozygous 455T→G (above) and 458A→T (below) changes. *D*, Dysmorphic facial features of individual 2 (with Asp153Val).

and exchange and the GTP hydrolysis.<sup>25</sup> Furthermore, two tracts, usually denoted as “Switch I” (residues 32–38) and “Switch II” (residues 59–67), undergo major conformational changes on GTP/GDP exchange and mediate binding to effectors, GAPs, and GEFs.<sup>24,26,27</sup>

Given the link between the functions of SHP-2 and RAS, we hypothesized that other genes encoding for proteins functioning as transducers in RAS signaling might be implicated in NS pathogenesis. Here, we report the identification of heterozygous *KRAS* gene mutations in a small percentage of subjects exhibiting a severe NS phenotype.

Eighty-seven subjects with NS and eight subjects with cardiofaciocutaneous (CFC) syndrome (MIM 115150) were included in the study. All the individuals were of European origin and lacked a *PTPN11* coding-sequence mutation<sup>12</sup> (M.T., B.D.G., and B.D., unpublished data). Informed consent for genetic analyses was obtained from all subjects considered in the study. For the vast majority of these individuals, clinical features satisfied diagnostic criteria for NS<sup>28</sup> and CFC syndrome,<sup>29</sup> but a few subjects who did not have features sufficient to make a definitive diagnosis were also considered. Genomic DNA was isolated from peripheral blood leukocytes, and the entire *KRAS* sequence coding for both the *KRASA* and the *KRASB* isoforms (exons 2–6) (fig. 1B) was screened for mutations. Primer pairs designed to amplify exons, exon/intron boundaries, and short intron flanking stretches are listed in table 1. The entire coding sequences of the *NRAS*, *HRAS*, and *DUSP6* genes, as well as the *NF1* genomic portion coding for the putative cysteine/serine-rich (exons 11–17)

and RASGAP (exons 21–27) domains of neurofibromin, were also screened for mutations. Primer sequences and PCR conditions are available on request. Mutation analysis of the amplicons was performed with denaturing high-performance liquid chromatography (DHPLC) by use of the Wave 2100 System (Transgenomic) at column temperatures recommended by Navigator software, version 1.5.4.23 (Transgenomic). Amplicons with abnormal denaturing profiles were purified (Microcon PCR [Millipore]) and were sequenced bidirectionally using the ABI BigDye Terminator Sequencing Kit v.1.1 (Applied Biosystems) and ABI Prism 310 Genetic Analyzer (Applied Biosystems). Paternity was confirmed by STR genotyping (AmpF/STR Identifier PCR amplification kit [Applied Biosystems]). Structural analyses and molecular graphics were performed using the program MOLMOL.<sup>30</sup>

Mutation analysis allowed the identification of heterozygous *KRAS* mutations in two individuals (fig. 1C). Both mutations were missense and affected exon 6, which encodes the C-terminal portion of *KRAS* isoform B.

A T→G transversion at position 455, predicting the substitution of Val<sup>152</sup> by a glycine residue (Val152Gly), was identified in a 1-year-old girl who had macrocephaly with high and broad forehead, curly and sparse hair, hypertelorism, strabismus, epicanthic folds, down-slanting palpebral fissures, hypoplastic nasal bridge with bulbous tip of the nose, high palate and macroglossia, low-set and posteriorly rotated ears, short neck with redundant skin, wide-set nipples, and umbilical hernia. She was born at 32 wk of gestation by cesarean section after a pregnancy

**Table 1. Primer Pairs and Annealing Temperatures ( $T_{\text{ann}}$ ) Used to Amplify the Entire *KRAS* Coding Sequence and the Size of PCR Products**

Exon	Primer Sequence (5'→3')		$T_{\text{ann}}$ (°C)	Product Length (bp)
	Forward	Reverse		
2	GATACACGTCTGCAGTCAACTG	GGTCCTGCACCAGTAATATGC	60	340
3	GGTGCACTGTAATAATCCAGACT	CATGGCATTAGCAAAGACTCA	56	300
4	GGTGTAGTGGAACTAGGAATTAC	GACATAACAGTTATGATTTTGCAAG	58	344
5 <sup>a</sup>	CTCAAGCTCATAATCTCAAACCTTCT	GTAGTTCTAAAGTGGTTGCCACC	58	305
6 <sup>a</sup>	GACAAAACACCTATGCGGATGA	GCTAACAGTCTGCATGGAGCA	62	429

<sup>a</sup> Exons 5 and 6 encode the C-terminal portions of *KRAS* isoforms A and B, respectively (fig. 1B).

complicated by a cystic hygroma detected at 12 wk and polyhydramnios at 30 wk. At birth, her weight was 2.550 kg (+3 SD), length was 43 cm (−0.5 SD), and head circumference was 32.5 cm (+2 SD), and she showed edema of lower limbs. Clinical examination at age 1 year showed severe failure to thrive because of poor intake, with weight, length, and head circumference at −5 SD, −5 SD, and +1 SD, respectively. No skin anomaly was noted, and no cardiac defect was documented by echocardiographic examination. The phenotype was compatible with a severe NS condition with features overlapping Costello syndrome (CS [MIM 218040]) (polyhydramnios, neonatal macrosomia and macrocephaly, loose skin, and severe failure to thrive) and, to a lesser extent, CFC syndrome (macrocephaly and sparse hair).

An A→T change at position 458, predicting the substitution of the adjacent aspartic acid residue by valine (Asp153Val), was observed in a 14-year-old girl with NS and some features of CFC syndrome (fig. 1D). She had short stature and growth retardation with delayed bone age, cardiac defects (moderate ventricular hypertrophy, mild pulmonic stenosis, and an atrial septal defect), dysmorphic features (hypertelorism, down-slanting palpebral fissures, strabismus, low-set and thick ears, relative macrocephaly with high forehead, and a depressed nasal bridge), short and mildly webbed neck, wide-set nipples, and developmental delay. There was hyperpigmentation of the skin and a large café-au-lait spot on the face. The creases of the hands and feet were deep. There was no keratosis or ichthyosis. The nails and teeth were normal. The hair was dry, thick, and without fracture and was wavy but not curly. Abnormalities of the extremities included cubitus valgus and joint hyperextensibility but not clinodactyly. Her gestation was complicated by polyhydramnios. She had feeding difficulties until age 4 years and subsequently experienced cyclic vomiting. She had a single seizure, at age 6 years. Application of the CFC index, a comprehensive scoring system developed to aid in diagnosing this disorder,<sup>29</sup> yielded a score of 9.483, which is just below the 5th percentile among patients with CFC.

Genotyping of parental DNAs confirmed paternity in both families and demonstrated the de novo origin of the mutations. Analysis of genomic DNA obtained from buccal cells of the affected individuals documented the oc-

currence of mutations, indicating that both lesions were germline events.

Val<sup>152</sup> and Asp<sup>153</sup> reside far from the portion of RAS typically altered in cancer,<sup>31</sup> which suggests a different pathogenetic mechanism for NS. To explore this, we used crystallographic information available on RAS family proteins. Although the crystallographic structure of *KRAS* per se has not been resolved, the available structures for other members of the RAS family are largely superimposable. The three-dimensional structures of HRAS (Protein Data Bank codes 4Q21 [for GDP-HRAS] and 5P21 [for GTP-HRAS]) were considered in our analysis because many structures of this protein have been resolved, including those of cancer-related mutants and complexes with GEF and GAP proteins. HRAS is 94% homologous to *KRAS* isoform B within the G domain.<sup>25</sup> In HRAS, a glutamic acid residue replaces Asp<sup>153</sup> in *KRAS*. We assumed, however, that the structure of this region was retained, because the substitution was conservative and Glu<sup>153</sup> and Asp<sup>153</sup> are almost equally represented among RAS proteins. Moreover, the structure of RRAS (Protein Data Bank code 2FN4), which has an aspartic acid residue at this position, shows almost no structural alteration (fig. 2A). The mutated residues Val<sup>152</sup> and Asp<sup>153</sup> are located at the N-terminus of the  $\alpha$ -helix ( $\alpha$ 5) spatially close to the G-5 region (residues 145–147)<sup>25</sup> (fig. 2B). The conformation of this region, which constitutes part of the guanine-binding pocket, is marginally affected by GDP/GTP switching (fig. 2C). The guanine binding is maintained by an H-bonding network involving residues Asp<sup>119</sup> and Ala<sup>146</sup>, which interact with the purine ring, and residues Gly<sup>13</sup>, Val<sup>14</sup>, Asn<sup>116</sup>, Lys<sup>117</sup>, Thr<sup>144</sup>, and Ser<sup>145</sup>, which strengthen those interactions. Val<sup>152</sup> and Asp<sup>153</sup> contribute to stabilizing the guanine-binding pocket. The side chain of Val<sup>152</sup> participates in the stabilization of a very tight hydrophobic core with residues Leu<sup>19</sup>, Leu<sup>23</sup>, and Ala<sup>146</sup> and the aliphatic chains of Gln<sup>22</sup> and Arg<sup>149</sup> (fig. 2B). The interactions with these amino acids strongly guide the orientation of the  $\alpha$ 5 helix and, as a consequence, of the loop containing the G-5 tract involved in the interaction with the purine ring. The introduction of a glycine residue at position 152 is predicted to affect the stability of that hydrophobic core. In addition, this change would endow the peptide chain with higher flexibility due to the presence of a Gly<sup>151</sup>Gly<sup>152</sup> mo-

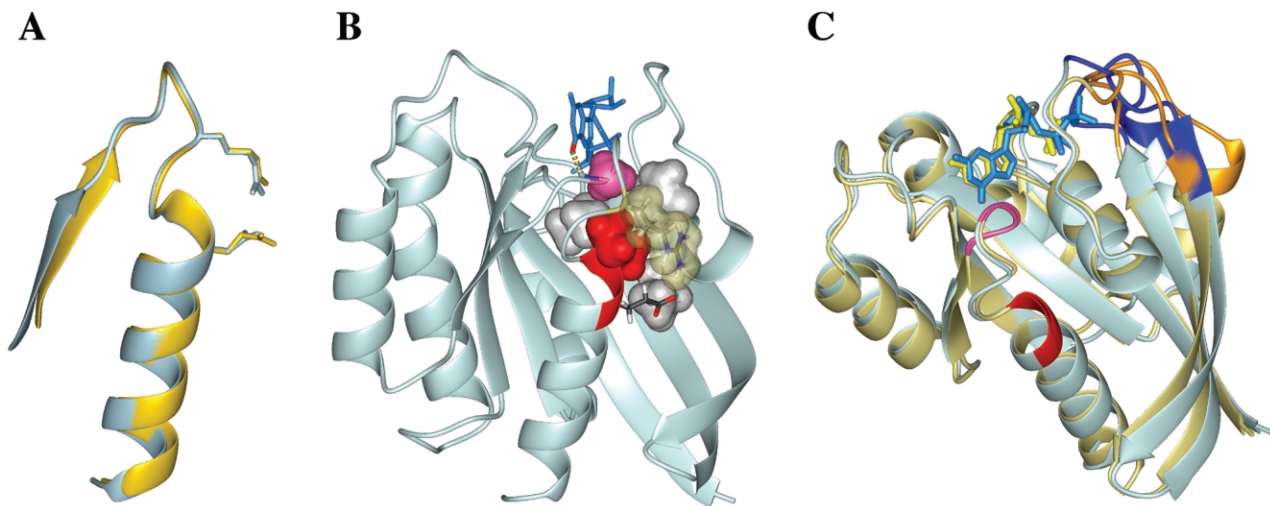


**Figure 2.** Structural analyses. *A*, Superimposition of the crystallographic structures of HRAS (yellow) and RRAS (light blue), in the region encompassing the  $\beta 6$  strand and  $\alpha 5$  helix. The side chain of HRAS residues Arg<sup>149</sup> ( $\beta 6$ - $\alpha 5$  loop) and Glu<sup>153</sup> ( $\alpha 5$ ) and the corresponding RRAS residues Arg<sup>176</sup> and Asp<sup>180</sup> are shown as a stick model. *B*, Crystallographic structure of GTP-HRAS<sup>32</sup> showing the interactions of residues 152 and 153. The side chain of Val<sup>152</sup> (red surface) participates in a hydrophobic core involving residues Leu<sup>19</sup>, Gln<sup>22</sup>, and Leu<sup>23</sup> (gray surfaces); Ala<sup>146</sup> (pink surface); and Arg<sup>149</sup> (semitransparent yellow surface). The side chains of residues 149 and 153, forming a salt bridge, are shown as a stick model. The yellow dashed line indicates the hydrogen bond formed by the N-H of the Ala<sup>146</sup> backbone and the O6 atom (red stick) of the GTP molecule (blue sticks). *C*, Superimposition of the crystallographic structures of GTP-HRAS<sup>32</sup> (light blue) and GDP-HRAS<sup>33</sup> (yellow) complexes. A ribbon representation is used for the protein backbone, whereas GDP and GTP are shown as a stick model. The positions of the mutated residues (N-terminus of the  $\alpha 5$  helix) and the G-5 motif are shown in red and pink, respectively. Regions assuming a different conformation in the two complexes (Switch I [residues 32–38] and Switch II [residues 59–67]) are shown in orange (in GDP-HRAS) and blue (in GTP-HRAS).

tif.<sup>34</sup> Glu<sup>153</sup> forms a salt bridge with Arg<sup>149</sup> (fig. 2B), an interaction that is retained in the comparable Asp residue in RRAS protein, with a shorter distance between the charged groups (fig. 2A). Loss of this salt bridge, caused by the Asp153Val mutation, is predicted to destabilize the conformation of the loop connecting the  $\alpha 5$  and  $\beta 6$  tracts (residues 144–151). Overall, these observations strongly indicate that the Val152Gly and Asp153Val substitutions destabilize the conformation of domains that contribute extensively to the interaction of KRAS with the GTP/GDP guanine ring and, consequently, are predicted to affect binding to both GTP and GDP. Since these residues are also involved in the binding of GTP-RAS with the human GEF protein SOS,<sup>35</sup> we cannot exclude the possibility that additional mechanisms, including disruption of possible regulatory interactions with GEF proteins, might also contribute to the pathological effects of these mutations. Since the 455T→G and 458A→T changes resided close to the splice-acceptor site, we considered the possibility of disruptive effects on an exonic splicing enhancer (ESE) site, using an informatics approach. ESEfinder analysis<sup>36</sup> identified a single site for the splicing factor SC35 (positions 13–20), which was not altered by these mutations. We cannot exclude the possibility that the mutations altered a site for an as-yet-unidentified ESE.

Following the discovery of *PTPN11* mutations as a major underlying cause of NS and LEOPARD syndrome,<sup>7,13,14</sup>

other developmental disorders clinically related to NS have been demonstrated to be caused by defects in genes that encode proteins functionally related to SHP-2, including *NF1* mutations and/or deletions in neurofibromatosis-Noonan syndrome (NFNS [MIM 601321]),<sup>37,38</sup> *HRAS* mutations in CS,<sup>39</sup> and, most recently, *BRAF*, *MEK1*, and *MEK2* mutations in CFC syndrome.<sup>40</sup> Here, we documented that *KRAS* gene mutations affecting *KRAS* isoform B can cause a severe form of NS, with a phenotype including features of CS and CFC syndrome. Studies published while our work was in review confirmed independently the causative role of *KRAS* mutations in NS and CFC syndrome pathogenesis.<sup>41,42</sup> Although the initial finding concerning *PTPN11* in NS implicated signaling downstream of RAS, it was unclear whether one or more pathways were affected. Taken together, the newer genetic findings specifically implicate perturbed signaling through the mitogen-activated protein kinase (MAPK) cascade. NS, LEOPARD syndrome, CFC syndrome, CS, and NFNS can now be grouped as developmental disorders resulting from mutations in functionally related genes. Although a significant portion of NS cases remain unexplained genetically, it appears highly likely that several additional genes related to RAS/MAPK signal transduction will ultimately be implicated.

*RAS* mutations associated with cancer generally upregulate *RAS* function by impairing the switch between the

active and inactive conformation, favoring a shift in the equilibrium toward the former.<sup>31,43,44</sup> The same is true of *HRAS* mutations causing CS<sup>39</sup> and a few *KRAS* mutations recently identified in NS<sup>42</sup> and CFC syndrome.<sup>41</sup> The NS-associated *KRAS* mutations described in this report, one of which was independently reported elsewhere,<sup>41,42</sup> are predicted to represent a novel gain-of-function mechanism. This appears to stem from an increased rate of GDP-GTP exchange related to a reduced affinity for GDP and GTP. This assertion is supported by biochemical data<sup>45–48</sup> from related RAS mutants characterized by substitutions involving residues Asn<sup>116</sup>, Asp<sup>119</sup>, and Thr<sup>144</sup>. In particular, biochemical and functional characterization of two *HRAS* mutants (Asp119Asn and Thr144Ile) demonstrated that an increase in rates of dissociation of GDP/GTP from the protein does not prevent the mutant RAS proteins from binding GTP in vivo and inducing transformation.<sup>49</sup> The mechanism leading to this gain-of-function effect has been characterized. Briefly, the inactive complex between wild-type RAS and GDP is normally stable, requiring interaction with GEF proteins for its dissociation. Mutations destabilizing the GDP-bound state favor spontaneous dissociation of this complex. In these mutants, unbound RAS tends to complex with GTP, because GDP and GTP have similar dissociation constants<sup>47</sup> but GTP has a significantly higher concentration in the cytoplasm (GTP:GDP ratio of 25:1).<sup>50</sup> On the basis of our structural analysis and these related biochemical data, we suggest that the Val152Ala and Asp153Val substitutions perturb the conformation of the guanine ring-binding pocket, increasing the GDP/GTP dissociation rate. This would shift the equilibrium toward the GTP-bound, active form and bypass the requirement for a GEF. These mutations would define a novel class of activating lesions that are inherited germline and that perturb development. To our knowledge, they have not been documented to occur as somatic lesions contributing to human hematologic malignancies or solid tumors. Functional studies to verify this hypothesis are in progress.

Both *KRAS* mutations identified in this study affected exon 6, which contributes to *KRASB* but not to *KRASA*.<sup>51</sup> *KRASA* and *KRASAB* differ at their C-termini, regions subjected to posttranslational modifications.<sup>52</sup> Similar to *HRAS* and *NRAS*, *KRASA* is palmitoylated at cysteine residues upstream of the conserved CAAX motif, which are replaced with a polylysine stretch in *KRAS* isoform B. This differential processing has profound functional effects, leading to alternative trafficking pathways to the plasma membrane and distinct membrane localization.<sup>51</sup> Recent evidence demonstrates that the two *KRAS* isoforms play distinct roles in development. While *KRASB* is ubiquitously expressed in embryonic and adult tissues, *KRASA* expression is restricted temporally and spatially and is not expressed in the adult heart.<sup>53</sup> Consistent with these data, loss of both *KRAS* isoforms is embryonic lethal,<sup>54,55</sup> whereas absence of only *KRASA* does not perturb development.<sup>53</sup> Although *KRAS* mutations affecting domains shared by the two isoforms can cause NS and CFC

syndrome,<sup>41,42</sup> the identification of exon 6 mutations documents that isolated *KRASB* gain of function is sufficient for disease pathogenesis—further evidence that *KRAS* isoform B plays the major role in development. Additional studies are required to delineate the phenotypic spectrum resulting from germline *KRAS* mutations as well as their molecular diversity and functional consequences for intracellular signaling and development.

## Acknowledgments

We are indebted to the patients and families who participated in the study and to referring physicians and colleagues who contributed samples to the investigators. This study was supported by Telethon-Italy grant GGP04172 and the Programma di Collaborazione Italia-USA/malattie rare (to M.T.); by National Institutes of Health grants HL71207, HD01294, and HL074728 (to B.D.G.); and by Italian Ministry of Health grant RC 2006 (to B.D.).

## Web Resources

Accession numbers and URLs for data presented herein are as follows:

ESEfinder Release 2.0, <http://rulai.cshl.edu/tools/ESE/index.html>  
Gene, <http://www.ncbi.nlm.nih.gov/entrez/query.fcgi?db=gene> (for *KRAS* genomic [accession number NC\_000012] and cDNA [accession numbers NM\_004985 and NM\_033360] sequences)  
Online Mendelian Inheritance in Man (OMIM), <http://www.ncbi.nlm.nih.gov/Omim/> (for NS, LEOPARD syndrome, CFC, CS, and NFNS)  
Protein Data Bank (PDB), <http://pdbeta.rcsb.org/pdb/Welcome.do> (for GDP-*HRAS* [code 4Q21], GTP-*HRAS* [code 5P21], and RRAS [code 2FN4] crystal structures)

## References

1. Noonan JA (1968) Hypertelorism with Turner phenotype: a new syndrome with associated congenital heart disease. *Am J Dis Child* 116:373–380
2. Noonan JA (1994) Noonan syndrome: an update and review for the primary pediatrician. *Clin Pediatr (Phila)* 33:548–555
3. Allanson JE (1987) Noonan syndrome. *J Med Genet* 24:9–13
4. Marino B, Digilio MC, Toscano A, Giannotti A, Dallapiccola B (1999) Congenital heart diseases in children with Noonan syndrome: an expanded cardiac spectrum with high prevalence of atrioventricular canal. *J Pediatr* 135:703–706
5. Tartaglia M, Gelb BD (2005) Noonan syndrome and related disorders: genetics and pathogenesis. *Annu Rev Genomics Hum Genet* 6:45–68
6. Jamieson CR, van der Burgt I, Brady AF, van Reen M, Elswi MM, Hol F, Jeffery S, Patton MA, Mariman E (1994) Mapping a gene for Noonan syndrome to the long arm of chromosome 12. *Nat Genet* 8:357–360
7. Tartaglia M, Mehler EL, Goldberg R, Zampino G, Brunner HG, Kremer H, van der Burgt I, Crosby AH, Ion A, Jeffery S, Kalidas K, Patton MA, Kucherlapati RS, Gelb BD (2001) Mutations in *PTPN11*, encoding the protein tyrosine phosphatase SHP-2, cause Noonan syndrome. *Nat Genet* 29:465–468
8. Neel BG, Gu H, Pao L (2003) The “Shp”ing news: SH2 domain-containing tyrosine phosphatases in cell signaling. *Trends Biochem Sci* 28:284–293
9. Tartaglia M, Kalidas K, Shaw A, Song X, Musat DL, van der

- Burgt I, Brunner HG, Bertola DR, Crosby A, Ion A, Kucherlapati RS, Jeffery S, Patton MA, Gelb BD (2002) *PTPN11* mutations in Noonan syndrome: molecular spectrum, genotype-phenotype correlation, and phenotypic heterogeneity. *Am J Hum Genet* 70:1555–1563
10. Fragale A, Tartaglia M, Wu J, Gelb BD (2004) Noonan syndrome-associated SHP2/*PTPN11* mutants cause EGF-dependent prolonged GAB1 binding and sustained ERK2/MAPK1 activation. *Hum Mutat* 23:267–277
  11. Keilhack H, David FS, McGregor M, Cantley LC, Neel BG (2005) Diverse biochemical properties of Shp2 mutants: implications for disease phenotypes. *J Biol Chem* 280:30984–30993
  12. Tartaglia M, Martinelli S, Stella L, Bocchinfuso G, Flex E, Cordeddu V, Zampino G, Burgt I, Palleschi A, Petrucci TC, Sorcini M, Schoch C, Foa R, Emanuel PD, Gelb BD (2006) Diversity and functional consequences of germline and somatic *PTPN11* mutations in human disease. *Am J Hum Genet* 78:279–290
  13. Digilio MC, Conti E, Sarkozy A, Mingarelli R, Dottorini T, Marino B, Pizzuti A, Dallapiccola B (2002) Grouping of multiple-lentiginos/LEOPARD and Noonan syndromes on the *PTPN11* gene. *Am J Hum Genet* 71:389–394
  14. Legius E, Schrandt-Stumpel C, Schollen E, Pulles-Heintzberger C, Gewillig M, Fryns JP (2002) *PTPN11* mutations in LEOPARD syndrome. *J Med Genet* 39:571–574
  15. Kontaridis MI, Swanson KD, David FS, Barford D, Neel BG (2006) *PTPN11* (Shp2) mutations in LEOPARD syndrome have dominant negative, not activating, effects. *J Biol Chem* 281:6785–6792
  16. Tartaglia M, Niemeyer CM, Fragale A, Song X, Buechner J, Jung A, Hahlen K, Hasle H, Licht JD, Gelb BD (2003) Somatic mutations in *PTPN11* in juvenile myelomonocytic leukemia, myelodysplastic syndromes and acute myeloid leukemia. *Nat Genet* 34:148–150
  17. Tartaglia M, Martinelli S, Cazzaniga G, Cordeddu V, Iavarone I, Spinelli M, Palmi C, Carta C, Pession A, Arico M, Masera G, Basso G, Sorcini M, Gelb BD, Biondi A (2004) Genetic evidence for lineage- and differentiation stage-related contribution of somatic *PTPN11* mutations to leukemogenesis in childhood acute leukemia. *Blood* 104:307–313
  18. Loh M, Vattikuti S, Schubert S, Reynolds MG, Carlson E, Lieu W, Cheng JW, Lee CM, Stokoe D, Bonifas JM, Curtiss NP, Gotlib J, Meshinchi S, Le Beau MM, Emanuel PD, Shannon KM (2004) Mutations in *PTPN11* implicate the SHP-2 phosphatase in leukemogenesis. *Blood* 103:2325–2331
  19. Araki T, Mohi MG, Ismat FA, Bronson RT, Williams IR, Kutok JL, Yang W, Pao LI, Gilliland DG, Epstein JA, Neel BG (2004) Mouse model of Noonan syndrome reveals cell type- and gene dosage-dependent effects of *Ptpn11* mutation. *Nat Med* 10:849–857
  20. Chan RJ, Leedy MB, Munugalavada V, Voorhorst CS, Li Y, Yu M, Kapur R (2005) Human somatic *PTPN11* mutations induce hematopoietic cell hypersensitivity to granulocyte-macrophage colony stimulating factor. *Blood* 105:3737–3742
  21. Mohi MG, Williams IR, Dearolf CR, Chan G, Kutok JL, Cohen S, Morgan K, Boulton C, Shigematsu H, Keilhack H, Akashi K, Gilliland DG, Neel BG (2005) Prognostic, therapeutic, and mechanistic implications of a mouse model of leukemia evoked by Shp2 (*PTPN11*) mutations. *Cancer Cell* 7:179–191
  22. Schubert S, Lieu W, Rowe SL, Lee CM, Li X, Loh ML, Clapp DW, Shannon KM (2005) Functional analysis of leukemia-associated *PTPN11* mutations in primary hematopoietic cells. *Blood* 106:311–317
  23. Bourne HR, Sanders DA, McCormick F (1991) The GTPase superfamily: conserved structure and molecular mechanism. *Nature* 349:117–127
  24. Mitin N, Rosmann KL, Der CJ (2005) Signaling interplay in Ras superfamily function. *Curr Biol* 15:R563–R574
  25. Wennemberg K, Rossman KL, Der CJ (2005) The Ras superfamily at a glance. *J Cell Sci* 118:843–846
  26. Barbacid M (1987) *ras* Genes. *Ann Rev Biochem* 56:779–827
  27. Hermann C (2003) Ras-effector interactions: after one decade. *Curr Opin Struct Biol* 13:122–129
  28. van der Burgt I, Berends E, Lommen E, van Beersum S, Hamel B, Mariman E (1994) Clinical and molecular studies in a large Dutch family with Noonan syndrome. *Am J Med Genet* 53:187–191
  29. Kavamura MI, Peres CA, Alchorne MM, Brunoni D (2002) CFC index for the diagnosis of cardiofaciocutaneous syndrome. *Am J Med Genet* 112:12–16
  30. Koradi R, Billeter M, Wuthrich K (1996) MOLMOL: a program for display and analysis of macromolecular structures. *J Mol Graph* 14:51–55
  31. Wittinghofer A, Waldmann H (2000) Ras-A molecular switch involved in tumor formation. *Angew Chem Int Ed* 39:4192–4214
  32. Pai EF, Kregel U, Petsko GA, Goody RS, Kabsch W, Wittinghofer A (1990) Refined crystal structure of the triphosphate conformation of H-ras p21 at 1.35 Å resolution: implications for the mechanism of GTP hydrolysis. *EMBO J* 9:2351–2359
  33. Milburn MV, Tong L, deVos AM, Brunger A, Yamaizumi Z, Nishimura S, Kim SH (1990) Molecular switch for signal transduction: structural differences between active and inactive forms of protooncogenic ras proteins. *Science* 247:939–945
  34. Venanzi M, Gatto E, Bocchinfuso G, Palleschi A, Stella L, Formaggio F, Toniolo C (2006) Dynamics of formation of a helix-turn-helix structure in a membrane-active peptide: a time-resolved spectroscopic study. *Chem Bio Chem* 7:43–45
  35. Margarit SM, Sondermann H, Hall BE, Nagar B, Hoelz A, Pirruccello M, Bar-Sagi D, Kuriyan J (2003) Structural evidence for feedback activation by RAS-GTP of Ras-specific nucleotide exchange factor SOS. *Cell* 112:685–695
  36. Cartegni L, Wang J, Zhu Z, Zhang MQ, Krainer AR (2003) ESEfinder: a web resource to identify exonic splicing enhancers. *Nucleic Acids Res* 31:3568–3571
  37. Baralle D, Mattocks C, Kalidas K, Elmslie F, Whittaker J, Lees M, Ragge N, Patton MA, Winter RM, French-Constant C (2003) Different mutations in the *NF1* gene are associated with neurofibromatosis-Noonan syndrome (NFNS). *Am J Med Genet A* 119:1–8
  38. De Luca A, Bottillo I, Sarkozy A, Carta C, Neri C, Bellacchio E, Schirinzi A, Conti E, Zampino G, Battaglia A, Majore S, Rinaldi MM, Carella M, Marino B, Pizzuti A, Digilio MC, Tartaglia M, Dallapiccola B (2005) *NF1* gene mutations represent the major molecular event underlying neurofibromatosis-Noonan syndrome. *Am J Hum Genet* 77:1092–1101
  39. Aoki Y, Niihori T, Kawame H, Kurosawa K, Ohashi H, Tanaka Y, Filocamo M, Kato K, Suzuki Y, Kure S, Matsubara Y (2005) Germline mutations in *HRAS* proto-oncogene cause Costello syndrome. *Nat Genet* 37:1038–1040
  40. Rodriguez-Viciana P, Tetsu O, Tidyman WE, Estep AL, Conger BA, Santa Cruz M, McCormick F, Rauen KA (2006) Germline

- mutations in genes within the MAPK pathway cause cardio-facio-cutaneous syndrome. *Science* 311:1287–1290
41. Niihori T, Aoki Y, Narumi Y, Neri G, Cave H, Verloes A, Okamoto N, Hennekam RC, Gillissen-Kaesbach G, Wiczorek D, Kavamura MI, Kurosawa K, Ohashi H, Wilson L, Heron D, Bonneau D, Corona G, Kaname T, Naritomi K, Baumann C, Matsumoto N, Kato K, Kure S, Matsubara Y (2006) Germline *KRAS* and *BRAF* mutations in cardio-facio-cutaneous syndrome. *Nat Genet* 38:294–296
  42. Schubbert S, Zenker M, Rowe SL, Boll S, Klein C, Bollag G, van der Burgt I, Musante L, Kalscheuer V, Wehner LE, Nguyen H, West B, Zhang KY, Sistermans E, Rauch A, Niemeyer CM, Shannon K, Kratz CP (2006) Germline *KRAS* mutations cause Noonan syndrome. *Nat Genet* 38:331–336
  43. Bos JL (1989) ras Oncogenes in human cancer: a review. *Cancer Res* 49:4682–4689
  44. Adjei AA (2001) Blocking oncogenic Ras signaling for cancer therapy. *J Natl Cancer Inst* 93:1062–1074
  45. Clanton DJ, Hattori S, Shih TY (1986) Mutations of the *ras* gene product p21 that abolish guanine nucleotide binding. *Proc Natl Acad Sci USA* 83:5076–5080
  46. Der CJ, Pan BT, Cooper GM (1986) *ras*<sup>H</sup> Mutants deficient in GTP binding. *Mol Cell Biol* 6:3291–3294
  47. Sigal IS, Gibbs JB, D'Alonzo JS, Scolnick EM (1986) Identification of effector residues and a neutralizing epitope of *H-ras*-encoded p21. *Proc Natl Acad Sci USA* 83:4725–4729
  48. Walter M, Clark SG, Levinson AD (1986) The oncogenic activation of human p21ras by a novel mechanism. *Science* 233:649–652
  49. Feig LA, Pan BT, Roberts TM, Cooper GM (1986) Isolation of ras GTP-binding mutants using an in situ colony-binding assay. *Proc Natl Acad Sci USA* 83:4607–4611
  50. Proud CG (1986) Guanine nucleotides, protein phosphorylation and the control of translation. *Trends Biochem Sci* 11:73–77
  51. Friday BB, Adjei AA (2005) K-ras as a target for cancer therapy. *Biochim Biophys Acta* 1756:127–144
  52. Silviu JR (2002) Mechanisms of Ras protein targeting in mammalian cells. *J Membr Biol* 190:83–92
  53. Plowman SJ, Williamson DJ, O'Sullivan MJ, Doig J, Ritchie AM, Harrison DJ, Melton DW, Arends MJ, Hooper ML, Patek CE (2003) While *K-ras* is essential for mouse development, expression of the *K-ras* 4A splice variant is dispensable. *Mol Cell Biol* 23:9245–9250
  54. Johnson L, Greenbaum D, Cichowski K, Mercer K, Murphy E, Schmitt E, Bronson RT, Umanoff H, Edelmann W, Kucheralapati R, Jacks T (1997) *K-ras* is an essential gene in the mouse with partial functional overlap with *N-ras*. *Genes Dev* 11:2468–2481
  55. Koera K, Nakamura K, Nakao K, Miyoshi J, Toyoshima K, Hatta T, Otani H, Aiba A, Katsuki M (1997) K-Ras is essential for the development of the mouse embryo. *Oncogene* 15:1151–1159